ORIGINAL ARTICLE

Witold Brostow · Victor M. Castaño
Alfonso Huanosta · Miguel de Icaza · Maria E. Nicho
José M. Saniger

Poly(acrylic acid) + zinc diacetate composites: High temperature service and electric conductivity

Abstract Poly(acrylic acid) + zinc diacetate hybrid composites have been prepared by precipitation from aqueous solutions and drying. The lowest glass transition temperature T_g determined by differential scanning calorimetry (DSC) is 392°C, providing a service temperature range unusually large for polymer-based materials (PBMs). Thermogravimetric analysis (TGA) shows that thermal decomposition begins some 10–20 K above each T_g. The alternating current impedance was determined in the nitrogen atmosphere from 370°C to 530°C. Dynamic dielectric measurements were performed between 20°C and 350°C, also under nitrogen. In contrast to typical PBMs, there is evidence of ionic conduction in some of the composites. The dynamic dielectric properties depend on the composition. The materials obtained are usable in medical applications and as high durability low friction coatings.

Witold Brostow (✉) · Victor M. Castaño (✉)
Department of Materials Science, University of North Texas,
Denton, TX 76230-5310, USA
e-mail: brostow@unt.edu, Fax: +1-940-565-4824,
http://www.unt.edu/LAPOM/

Victor M. Castaño (✉) · Miguel de Icaza
Department of Applied Physics and Advanced Technology,
National Autonomous University of Mexico,
Apartado postal 1-1010 Querétaro, Qro. 67000, Mexico
e-mail: meneses@servidor.unam.mx

Alfonso Huanosta
Institute of Materials Research,
National Autonomous University of Mexico,
Ciudad Universitaria, Mexico, D.F. 04510, Mexico

Maria E. Nicho
Institute of Electrical Research, Apartado postal 475,
Curenavaca, Morelos 62000, Mexico

José M. Saniger
Center for Instrumentation,
National Autonomous Universtiy of Mexico,
Ciudad Universitaria, Mexico, D.F. 04510, Mexico

1 Introduction

While a gradual conversion from metals and their alloys to polymer-based materials (PBMs) is taking place in industry, military and medicine, metals generally have service temperature ranges reaching much higher than polymers. The metal technology is also well established in applications such as coatings. Mass-produced engineering polymers (EPs) are typically flexible, mechanically not very strong, with high isobaric expansivities (thermal expansion coefficients) and usable in relatively narrow temperature ranges.

There are several approaches to achieving successful conversion from metal alloys to PBMs. One is the use of polyimides (PIs), including thermoplastic ones [1, 2]. Polymer liquid crystals (PLCs) constitute a second class of high-temperature polymers, with additional advantages of relative ease of processing, better mechanical properties than EPs, and low thermal expansivities [3, 4]. Among various chemical structures of PLCs, we have also those based on epoxies [5]. Moreover, blends of the PLC + PI type have also been successfully made [6, 7].

In this paper we are dealing with a still different class of high-temperature PBMs, so-called polyelectrolyte cements. While they have already found specific applications as dental cements [8–13] or biocompatible composites [14], optimization of their properties is difficult. Generally speaking, polyelectrolyte cements are obtained by reacting a metal oxide (MO) and a polyelectrolyte polymer (HA, typically polyacrylic acid), as follows:

$$MO + 2HA \mapsto MA_2 + H_2O \qquad (1)$$

There exists literature on characterization of the products of this reaction [8–10] and also on the reaction mechanism studied by spectroscopic techniques [11, 12]. From the Materials Science point of view, such a material is a compound and a composite at the same time; due to dif-

fusion limitations there is always a portion of unreacted metal oxide. Given the combination of a polymeric and a non-polymeric constituent, the name *hybrid composites* seems appropriate.

Detailed kinetics of reaction (1) is difficult to determine; this not only because of the unreacted MO but also because polyacrylic acid (a substrate) is soluble in water (a product). The possibility of producing a polymer + metal composite at the room temperature, entirely reacted, is not only attractive intellectually but also represents an opportunity to produce new PBMs with properties pertinent for applications in a number of technological fields. In this article we report the development of a novel material, related to the polyelectrolyte cements defined above. Our material is the product of a reaction between polyacrylic acid and zinc acetate, that is, a liquid-liquid reaction, instead of the liquid-solid reaction of a standard polyelectrolyte cement. Certain details of the sample preparation technique employed in this work have been reported before [15, 16].

2 Experimental

The starting materials for the preparation of the polyacrylic acid + zinc acetate composites (PAA + ZnAc) were: 25 wt. % aqueous solution of polyacrylic acid (number-average molecular mass $M_W = 2.5 \cdot 10^4$, Aldrich Chemical Co.); and reactive grade $Zn(CH_3COO)_2 \cdot H_2O$ and $ZnCl_2$ (both Baker). The method consists essentially in manually stirring at room temperature a mixture of the stoichiometric amounts of reacting solutions until a powdery precipitate is formed. All the precipitates are first dried under room conditions and then at 423 K.

Three samples so obtained were selected for further studies. Sample I was obtained by reacting the stoichiometric amount of 0.1 M aq. solution of PAA and $Zn(CH_3COO)_2$. Samples II and III were prepared by reacting stoichiometric amounts of 0.1 M aq. sodium polyacrylate (NaPA) with 0.1 M aqueous solutions of respectively $Zn(CH_3COO)_2$ or $ZnCl_2$. The sodium polyacrylate solution was prepared by dropping 0.5 M aq. NaOH into PAA until pH = 7 was reached. Sample I precipitated in the form of gel while samples II and III precipitate as fine powders. This difference can be related to different molecular conformations of PAA and NaPA. NaPA does not contain hydrogen bonds and has, therefore, fairly open macromolecular structures; little water is trapped and powder precipitates are produced. By contrast, hydrogen bonds are present in PAA – what results in the tendency to a globular arrangement of the molecule, trapping a high amount of water, and the resulting gel-like appearance of the ZnPAA precipitate. Table 1 shows the Zn contents of the precipitates after drying at 423 K determined by atomic absorption spectroscopy, along with the final stoichiometry of each of them.

Thermophysical characteristics of the samples was determined by differential scanning calorimetry (DSC) and thermogravimetric analysis (TGA) using TA instruments.

We have determined ac impedance Z of the composites in the form of disc-shaped pellets. The dried samples were ground to fine powders and pressed at 7000 kg/cm² to obtain the pellets (12 mm in diameter and 1 mm thick). Vacuum-sputtered gold electrodes were placed on each face of each pellet, resulting in a sandwich-like structure gold-composite-gold. The discs were connected with gold strips to platinum wires and placed inside a computer-controlled furnace with nitrogen atmosphere. Initially, the samples were kept at the desired temperature (within ± 3 K) for 30 minutes to achieve thermal equilibrium. Then the impedance measurements were carried out, covering the temperature range from 633 to 803 K. The data were recorded over the frequency range from 5 Hz to 13 MHz by using a computer-controlled Hewlett-Packard HP4192 A impedance analyzer. The applied voltage was 1 V in all cases.

Finally, we have also made dynamic dielectric experiments using a dielectric analyzer (TA Instruments DE 2970). At isothermal conditions, the complex dielectric permittivity ε* is

$$\varepsilon^*(f) = \varepsilon'(f) - i \cdot \varepsilon''(f) \qquad (2)$$

where f is the frequency, ε' is the real part, ε'' is the imaginary part while $i = (-1)^{1/2}$. For these tests, fine powders were deposited on a ceramic single surface sensor with gold electrodes. A constant force of 400 kg was applied throughout the experiments. Twenty-eight different frequencies were scanned in the range from 0.1 Hz to 300 kHz. The experiments were conducted under nitrogen atmosphere, between room temperature and 623 K, at the heating rate of 3 K/minute with the applied voltage of 1 V.

3 Thermophysical characteristics

The glass transition temperatures T_g obtained by DSC and the temperatures T_h seen in TGA when the thermal decomposition begins are listed in Table 2. We note that the lowest glass transition temperature is T_g = 665 K (= 392°C) for sample I. Thus, our objective of creating PMBs with a large service temperature range has been largely achieved. The decomposition begins some 10–20 K above the glass transition, depending on the sample composition.

4 Impedance and dielectric properties

Usually, ac impedance results are displayed on the complex impedance Z* plane described by

$$Z^* = Z' - iZ'' \qquad (3)$$

the real and imaginary parts being respectively Z' and Z'' while Eq. (3) is an evident analog of Eq. (2). Then the impedance data can be conventionally analyzed in terms of equivalent circuits [17] by networks of resistance R and capacitance C elements connected in different arrays. The appropriate equivalent circuit is selected according to a predefined working hypothesis based on expected physical behavior within the system. The ac impedance spectra have the appearance of a single large semicircle fol-

Table 1 Compositions of Composites

Sample number	Zn % (weight)	Zn % (atomic)	Residual elements and their % atomic conc.	Proposed stoichiometry
Sample I	28.68	91	H / 9	$(Zn_{0.91}H_{0.18}(acrylate)_2)_n$
Sample II	30.29	96	Na / 4	$(Zn_{0.96}Na_{0.08}(acrylate)_2)_n$
Sample III	31.32	99	Na / 1	$(Zn_{0.99}Na_{0.02}(acrylate)_2)_n$
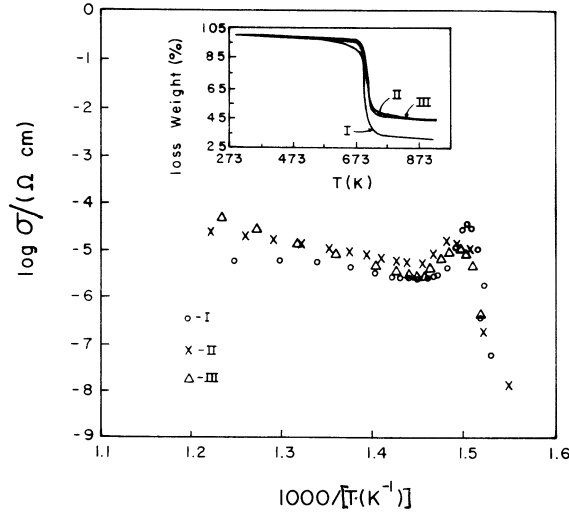
Fig. 1 Electrical conductivity vs. inverse temperature for all samples. Weight loss vs. temperature for the same samples in the insert

Table 2 Glass transition temperatures T_g and thermal decomposition threshold temperatures T_h

| Sample number	T_g/K	T_h/K
I	665	683
II	677	686
III	669	684

lowed at low frequencies by a small arc. This scheme was observed for our samples over the full range of temperatures studied. Thus, the experimental situation can be simulated by an equivalent circuit formed by two parallel RC elements connected in series, each of them described by an associated impedance given by

$$Z = (1/R_b - i\omega\, C_b)^{-1} \qquad (4)$$

R_b and C_b are here the common resistor and capacitor elements, ω is the angular frequency defined by $\omega = 2\pi f$ while f is the measured frequency. As it will be shown later, the large semicircle characterizes the electrical behavior of the bulk of the sample whereas the small one reflects electrode phenomena. The assignment is based on the magnitude of the associated capacitance. The dielectric parameters of the studied compounds have, therefore, been determined from the larger semicircle. In that case, the low frequency intercept of the semicircle on the real component Z' axis provides the value RC through the condition $\omega_{max}RC = 1$ which corresponds to the maximum of the semicircle.

Experimental R values were used to calculate the associated conductivity through the relation $\sigma = g_f/R_b$, where g_f is a geometrical factor which take care of the shapes and sizes of the samples and electrodes. Thus, plots of log σ vs. 1000/(T/K) can be drawn – as shown in Fig. 1. A sharp maximum is observed about 1000/(T/K) = 1.50, which is approximately 390°C. A further temperature increase lowers the conductivity until a minimum reached at about 420°C. Afterwards an approximately linear increase in conductivity is observed.

The dependence displayed in Fig. 1 obviously does not correspond to the classical Arrhenius behavior where a linear relation between the logarithmic conductivity and inverse temperature is expected. However, the deviations from the Arrhenius behavior are useful; they provide us with certain clues on mechanisms producing the observed dielectric behavior. Thus, the temperature at

which the minimum in conductivity is reached agrees within a few degrees with the decomposition threshold temperatures T_h observed for the ZnPA compounds by thermogravimetric analysis and reported in Table 2. Similarly, the abrupt change of the slope already mentioned which occurs before the T_h, namely around 390°C, may be associated with the glass transition (see again Table 2) at which changes in the electrical behavior of our hybrid composites must be expected. We recall in this context the results of Sawaby and coworkers [18] who report that there are no glass transitions for their polyacrylate cements below 300°C.

The fact that the glass transition temperatures obtained following two so different routes agree well allows us to make a calculation of the approximate activation energy E_a necessary to move charge carriers or dipoles within the system. The resulting E_a value, approximately 20 eV, will be discussed later on. If a linear behavior below the lowest experimental registered temperatures is assumed, then the activation energy will be related to the dielectric process taking place in the composite. This assumption is supported by the observed thermal behavior shown in the insert to Fig. 1. There the weight loss as function of temperature determined by TGA shows a nearly horizontal (descending slightly) region below the glass transition temperature T_g. The high value of the activation energy for that region reflects probably the stiffness of the molecular groups in the material.

As for processes which occur above the temperature T_h which is the threshold of thermal decomposition, they correspond to the gradual transformation of Zn + PA into ZnO. This explanation is also compatible with the thermogram in the insert to Fig. 1: weight loss becomes significant when the decomposition is taking place. Above T_h the increasing thermal energy can give rise to an additional electronic component to the total conductivity. For our purposes this region is unimportant, however.

The capacitance values for our composites are of the order of pF (picofarads). Alternating current impedance measurements have an advantage that different regions present in a material (bulk, secondary phases, grain boundaries, etc.) produce each a characteristic capacitance value. As already pointed out by Irvine and coworkers [19], it is for this reason that the relaxation responses associated with each region are strongly frequency-dependent. The same authors note that typical capacitance for the bulk of polyelectrolyte cements must be of the order of pF. Our calculations based on the data for the large semicircle lead to comparable numbers.
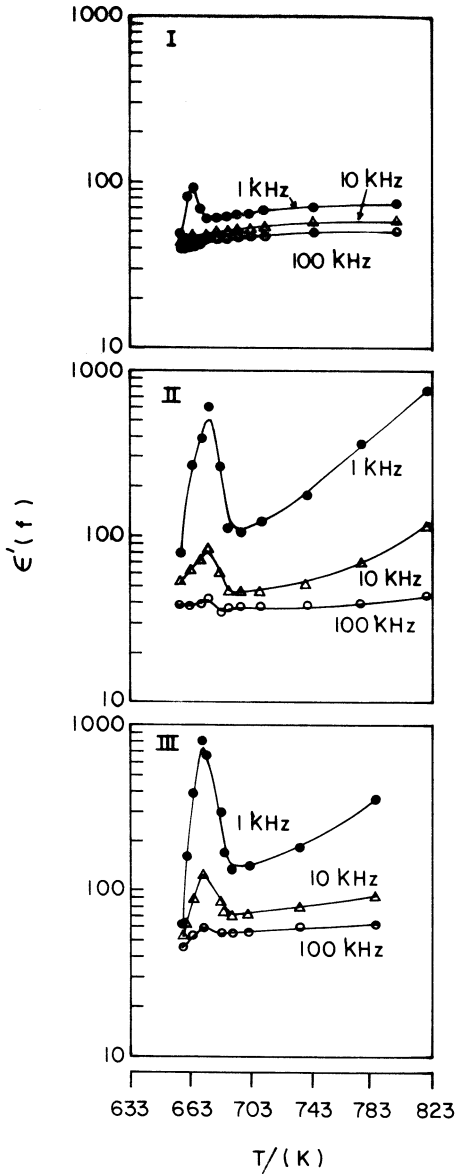
Fig. 2 The storage (real) component ε' of the complex dielectric permitivity vs. temperature for each sample at several frequencies

The standard relation between the capacitance C_b and the relative dielectric permittivity (dielectric constant) is $\varepsilon = g_f C_b / \varepsilon_o$ where the already mentioned geometrical factor $g_f = d/A$; d is the thickness of the sample, A the surface area of the sample (here gold-sputtered) and ε_o is the permittivity of the vacuum. One expects that C_b values are independent of frequency. Calculations based on our experimental data for the bulk materials confirm that this is indeed the case. However, given the relation between C_b and ε, the capacitance values can well vary with the temperature. Our ε results have been obtained for a series of temperatures. Nevertheless, it turns out that the experimental dielectric constants are independent of the preparation procedure as well as independent of temperature. Consequently, the capacitance values do not depend on the temperature either.

Returning now to Eq. (2), the real (storage) part ε' of the complex dielectric permittivity is typically frequency-dependent. In Fig. 2 we present ε' results as a function of temperature for all three samples studied, in each case as a family of curves for several frequencies f. Clear peaks are observed at low frequencies for all samples. ε'(f, T) has a maximum value of 800 at f = 1 kHz for samples II and III while the corresponding value for sample I is considerable smaller. At higher frequencies, however, ε'(f,T) shows an almost constant value of around 60 for all the samples. Thus, samples II and III are more strongly polar than sample I, especially so for low frequencies (1 and 10 kHz). The ε' plots have strong resemblance to the corresponding conductivity plots, confirming the importance of both T_g and T_h temperatures for the electrical behavior of the samples.

When ionic charge carriers move within a material, the corresponding impedance spectrum often contains inclined spikes at low frequencies [19], this in addition to the circular arcs. In this situation appropriate equivalent circuits are those formed by a series of arrays of parallel RC elements; a capacitance C_p represents the blocking effects at the sample/electrode interface. Expected values of C_p can vary in a wide range, from 10^{-7} to 10^{-5} F [18]. In our case, the experimental data do not show a well defined spike in the Z" vs Z' plane, despite the fact that the capacitance of the second semicircle, of the order of μF, is typical for interfacial polarization. Since the data have the locus of a small arc instead of a vertical spike, it can be concluded that the electrode response is not really impeding; instead, we have a relatively small charge transfer resistance. That resistance can be explained by the presence of a fairly number of thermally-activated electronic charge carriers. At the same time, the calculated C_p values confirm the existence of ionic motion.

Movements of ions have been ascribed in the literature to polarization processes that are thermally activated. Thus, a dipole movement of some kind is taking place. The respective process can be characterized by a time constant τ. The constant is generally temperature-dependent and represents the dielectric reorientation that takes place. On the other hand, the reorientation can also be represented by an exponential distribution of the activation energies E_a. There are two more specific interpretations of the reorientation time τ. According to one, τ represents the time an ion needs to diffuse across the average separation of favorable sites in the bulk of the material. Alternatively, τ is associated with the time spent in a dipole reorientation during the relaxation process.

Calculated τ values are plotted in Fig. 3 as a function of temperature. They represent an approximate linear dependence below the glass transition temperature – typical for a thermally-activated Arrhenius process. Values of T_g obtained from these plots are consistent with those found in Fig. 1 and also those determined by DSC and reported in Table 2. As noted earlier, for T <
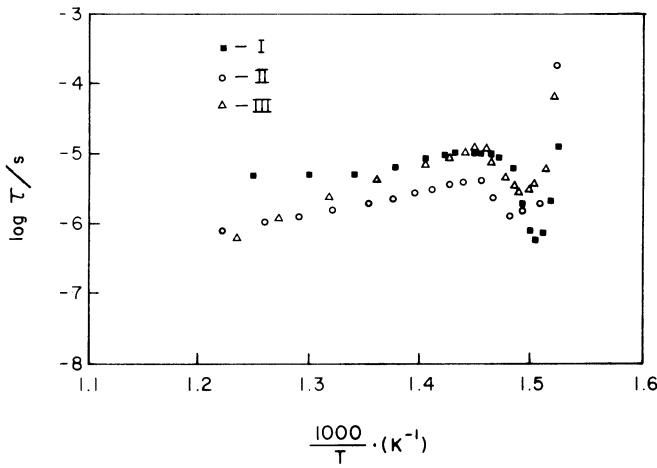
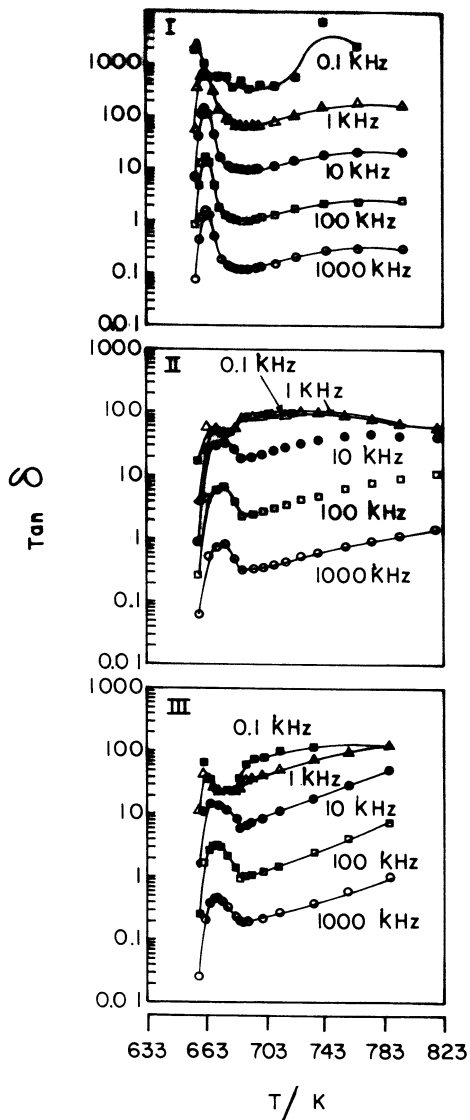**Fig. 3** Logarithmic relaxation time log τ vs. inverse temperature for all samples

Fig. 4 Dielectric tan δ vs. temperature for each sample at several frequencies
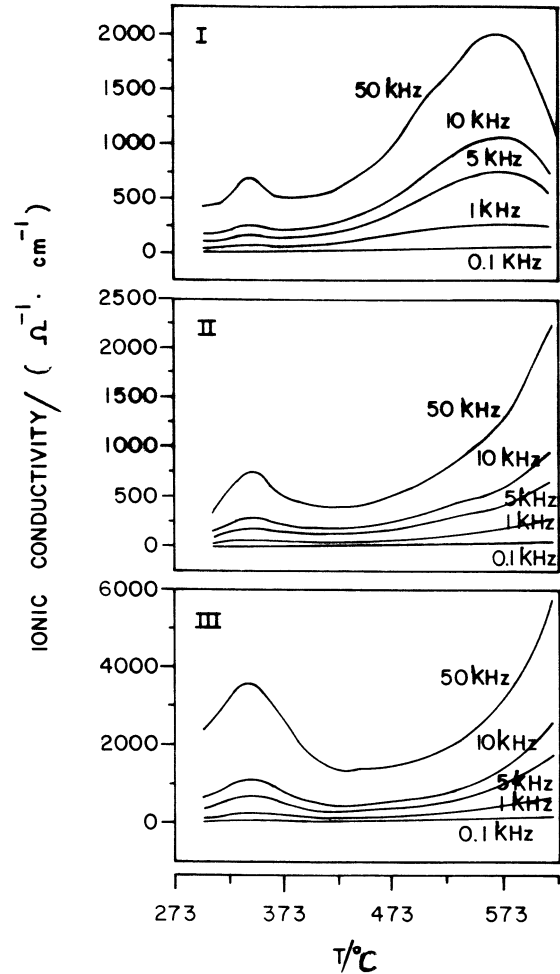

Fig. 5 Ionic conductivity vs. temperature for all samples

T_g we have estimated the activation energy for the process and found E_a amounting to approximately 20 eV, a relatively large number. This clearly reflects non-equilibrium events such as changes in the conformations of the chains, or cooperative motions occurring in the material. We recall, therefore, that stress relaxation has been explained by Kubát and coworkers as a cooperative process [20–22] involving clusters of chain segments in polymers (or individual atoms in metals). The Kubát theory has been confirmed by molecular dynamics computer simulations [23, 24]. The processes reflected by the large value of the activation energy appear to be the precursors of the glass transition. Raising the temperature produces a thermally-activated phenomena above T_h, which clearly correspond to those observed in Fig. 1.

In Fig. 4 we show plots of the absolute values of the dielectric tan δ = ε"/ε' vs. temperature at selected frequencies for all samples. While we have results at other frequencies, the results displayed are representative for the behavior. For each sample, the temperature at which the sharp maximum occurs is independent of the frequency, agrees with the maximum in the log σ vs. 1000/(T/K)
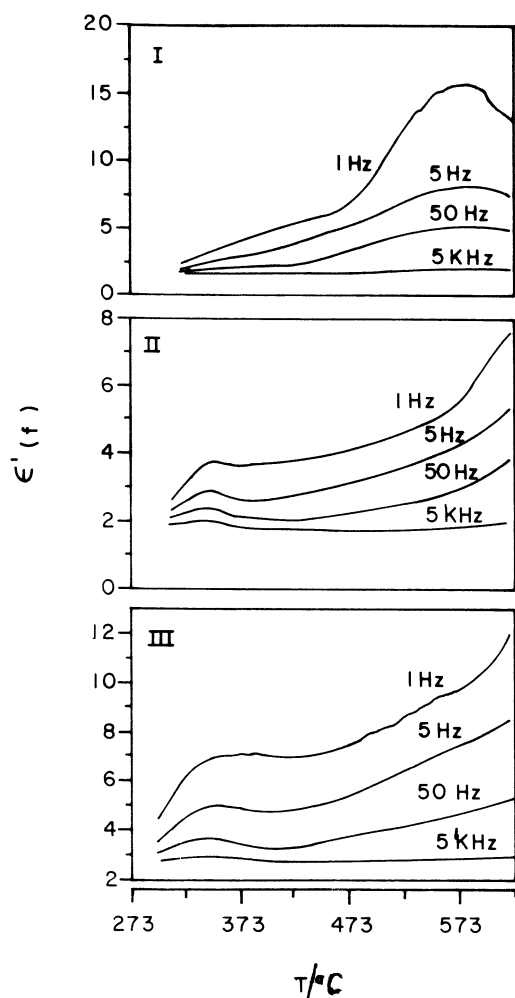
Fig. 6 The storage (real) component ε' of the complex dielectric permitivity vs. temperature for all samples from the room temperature up to 350°C

plots in Fig. 1, and also agrees with the glass transition temperature determined by calorimetry. The frequency dependence of tan δ is more evident at low frequencies. The relatively high values of tan δ at those frequencies reflect ion migration phenomena which constitute a source of energy loss – thus producing high loss factor ε'' values.

As said in Section 2, dynamic dielectric experiments were carried for all samples between the room temperature and 623 K. Using a Drude model, values of ionic conductivity have been calculated and are shown in Fig. 5 plotted against temperature. The composites II and III exhibit two intervals of temperature where movements of ions are present. These experimental results confirm the previous assertion on the existence of ionic charge carriers. On the other hand, in compound I there exists a relatively broad maximum at around 323–333 K, and a second one at about 573 K. In all our hybrid composites we thus have evidence of ionic conduction.

The temperature dependence of the permittivity at four frequencies is shown in Fig. 6 for each of the samples. Each curve shows a relatively broad maximum be-

tween 323–373 K, reflecting the existence of a non-negligible internal polarization. A second maximum is observed at temperatures around 523 K. It can be attributed to an α-type solid state relaxation mechanism combined perhaps with motions of ions between relatively long macromolecular chains.

5 Concluding remarks

Our quest for polymer-based materials with the service range extending to high temperatures has led us to polycrylic acid + zinc acetate hybrid composites with high glass transiton temperatures. In contrast to already known polyacrylate cements, our synthesis occurs in liquid media only, without solid substrates. The fact that the medium is aqueous suggests applications as coatings – without the use of organic solvents still so typical for polymeric coatings. In contrast to typical inorganic cements, our composites exhibit smooth surfaces – one more advantage in potential coating applications.

The dielectric character of the samples presents minor variations depending on the synthesis pathway. The samples obtained directly from PAA show lower values of the dielectric parameters than those obtained from NaPA. The evidence of ionic conduction opens a separate area of potential applications.

Variations in compositions of the substrates provide the capability of controlling properties of our new materials. Much remains to be done, including tribological studies (friction, adhesion, wear) of our composites on various substrates. We hope to report more results later on.

References

1. Narkis M, Rosenzweig N (eds) (1995) Polymer Powder Technology. Wiley, Chichester New York
2. Feldman D, Barbalata A (1996) Synthetic Polymers: Technology, Properties and Applications. Chapman & Hall, London
3. Brostow W (1996) In: Mark JE (ed) Physical Properties of Polymers Handbook. American Institute of Physics Press, Woodbury, New York, chap 33
4. Brostow W (ed) (1998) Mechanical and Thermophysical Properties of Polymer Liquid Crystals. Chapman & Hall, London
5. Giamberini M, Amendola E, Carfagna C (1995) Molec Cryst Liq Cryst 266: 9
6. Brostow W, D'Souza NA, Gopalanarayanan B (1998) Polymer Eng & Sci 38: 204
7. Brostow W, D'Souza NA, Gopalanarayanan B, Jacobs EG (1999) Polymer Eng & Sci 39: (in press)
8. Hill RG, Labok SA (1991) J Mater Sci 26: 69

9. Nicholson JW, Hawking SJ, Wasson EA (1993) J Mater Sci Med 4: 32 (and references therein)
10. Padilla A, Martínez JL, Sánchez A, Castaño VM (1992) Mater Lett 12: 445
11. Saniger J, Hu H, Castaño VM (1992) Mater Lett 15: 113
12. Hu H, Saniger J, García-Alejandre J, Castaño VM (1991) Mater Lett 12: 281
13. Nicholson JW, Wilson AD (1987) Brit Polymer J 19: 67
14. Vélez D, Arita IH, García-Garduño MV, Castaño VM (1994) Mater Lett 19: 309
15. Nicho ME (1995) MS Thesis in Materials Science. National Autonomous University of Mexico, Mexico City
16. Nicho ME, Saniger J, Ponce M, Huanosta A, Castaño VM (1997) J Appl Polymer Sci 66: 861
17. McDonald JR (1987) Impedance Spectroscopy. Wiley, New York
18. Sawaby A, Moharam MA, Tahon KH (1988) J Mater Sci Lett 7: 1166
19. Irvine JTS, Sinclair DC, West AR (1990) Adv Mater 2: 132
20. Kubát J (1982) Phys Status Solidi B 111: 599
21. Kubát J, Nilsson LÅ, Rychwalski W (1982) Res Mechan 5: 309
22. Kubát J, Rigdahl M (1986) In: Brostow W (ed) Failure of Plastics. Hanser, Munich, chap 4
23. Brostow W, Kubát J (1993) Phys Rev B 47:7659
24. Blonski S, Brostow W, Kubát J (1994) Phys Rev B 49: 6494